JOURNAL OF CHEMICAL INFORMATION AND MODELING

Article

pubs.acs.org/jcim

Dynamics of hERG Closure Allow Novel Insights into hERG Blocking by Small Molecules

Peter Schmidtke,[†,‡] Marine Ciantar,[†] Isabelle Theret,[†] and Pierre Ducrot*[,†]

[†]Institut de Recherches Servier, 125 Chemin de Ronde, 87290 Croissy-sur-Seine, France

[‡]Discngine, 33 Rue du Faubourg Saint-Antoine, 75011 Paris, France

Supporting Information

ABSTRACT: Today, drug discovery routinely uses experimental assays to determine very early if a lead compound can yield certain types of off-target activity. Among such off targets is hERG. The ion channel plays a primordial role in membrane repolarization and altering its activity can cause severe heart arrhythmia and sudden death. Despite routine tests for hERG activity, rather little information is available for helping medicinal chemists and molecular modelers to rationally circumvent hERG activity. In this article novel insights into the dynamics of hERG channel closure are described. Notably, helical pairwise closure movements have been observed. Implications and relations to hERG inactivation are presented. Based on these dynamics novel insights on hERG blocker placement are presented, compared to literature, and discussed. Last, new evidence for horizontal ligand positioning is shown in light of former studies on hERG blockers.

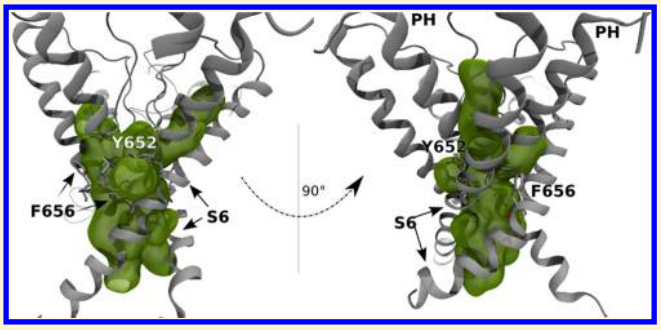

INTRODUCTION

Research during the last decades helped to gather information for a better understanding of the functioning of ion channels. Among others, especially the KCNH2 gene and the corresponding *human-ether-à-go-go* (hERG) protein attracted much attention due to its important physiological role. hERG is responsible for the delayed rectifier K^+ current (I_{Kr}). This current is necessary for membrane repolarization and activated upon membrane depolarization. The KCNH2 gene is expressed in a variety of tissues (i.e., brain and heart), but expression and function of the hERG protein is best characterized in cardiac myocytes. Malfunction of the channel can cause deathly heart arrhythmia, often characterized by long QT intervals (time from initial membrane depolarization to final repolarization). Such long QT intervals can be caused by mutations in the hERG channel[1] but also by the binding of small molecules to the protein.[2] The later raised major interest of the pharmaceutical industry for studying the influence of small molecules on the channel activity. Today, FDA guidelines (ICH S7B) expect nonclinical testing of new molecules for pro-arrhythmic risk and ventricular repolarization. Both are known to be linked to hERG activity. For this reason, high throughput functional assays exist to verify whether a molecule can alter hERG activity.[3] Furthermore, recent attempts try to identify molecules that lower hERG related drug induced arrhythmias.[4]

Despite the availability of biological assays (automated patch clamp and binding assays for example), theories on the mode of action and especially binding of hERG blockers have not yet found a sound consensus in the scientific community. Experimental assays can certainly give an answer about the action of a molecule on the channel function. However, it is still very difficult to derive guidelines for chemical synthesis from these results.

Theoretical approaches can help to gain deeper insights into these aspects. In the past, mainly ligand based techniques have been used to derive rules on what makes a molecule an active hERG blocker.[3] While QSAR models were shown to be able to predict hERG blocking activity, variability of prediction remained high between different data sets used.[5] Also, such models lack structural interpretation which is generally wanted for proposing sound synthesis guidelines for medicinal chemists. Next to various QSAR models a consensus pharmacophore of hERG blockers was described by different independent studies. This pharmacophore is composed of 3 hydrophobic/aromatic rings with a central charged amine.[6−10] Such models allowed the establishment of first hypotheses on how to lower hERG activity by chemical modifications on small molecules.

Studying hERG using structure based techniques was hindered by the lack of crystal structures of homologue ion channels. However, with the availability of first crystal structures for bacterial potassium channels homology modeling was then used to derive structural models of hERG. Sequence similarity between hERG and currently used templates remains below 30% and the built models have to be interpreted with great care. Despite this fact a multitude of structure based approaches were then used to propose hypotheses on the

Received: March 4, 2014
Published: July 7, 2014

   dx.doi.org/10.1021/ci5001373 | *J. Chem. Inf. Model.* 2014, 54, 2320−2333

binding mode of known hERG blockers but also on the functioning of the channel.

Structural modeling allowed for assessment of the different conformational states the channel can undergo during a full functional cycle, such as open, closed, and inactive states.[11] It is a sound assumption that hERG blockers enter the channel when in it's open state. However, it is still poorly understood and rarely questioned which state of the channel is more likely to tightly bind such small molecules. Very often the open state was modeled using homology modeling templates from the KvAP or KcsA channel resulting in a widely open and solvent accessible drug binding site below the selectivity filter.[12−15] It is however questionable if such an open conformation is ideal for prospective placement of small molecules and their subsequent scoring. It can also be discussed if such a state is even representative of the open state of the hERG channel. This issue has already been commented in previous studies.[16,17] More recent works[18−20] introduced the use of novel templates for modeling hERG, notably Kv1.2.[21] In contrast to KvAP or KcsA, here the resulting hERG model contains a narrower central cavity. Such a conformation is likely to allow for a closer fit to small molecules upon further equilibration.

Well known long QT syndrome inducing drugs like astemizole, cisapride, terfenadine, and sertindole are often used to analyze hERG channel block. Unfortunately, despite a plethora of works during the last years rather contradictory results have been published and still today no consensus on mode of action and binding mode of hERG blockers has been reached. Still today lots of studies assume that hERG blockers bind along the conduction pore axis (in parallel to the axis).[8,12,15,20,22]

The work presented throughout this paper intends to answer several of the previously exposed issues. In-silico techniques were used to describe the hERG closure motion and binding of hERG blockers. The transmembrane part of the hERG protein was modeled using the Kv2.1/Kv1.2 paddle chimera crystal structure[23] with a S4 helix shifted into cytoplasm corresponding to the closed state of the voltage sensitive domain. Molecular dynamics (MD) simulations allowed to simulate the beginning of the channel gate closure involving pairwise symmetric S6 and S5 helix bending events described in detail.

Dynamic events linked to hERG inactivation are described in detail and compared to literature.

In contrary to most of the previous studies, extraction of representative conformations along the trajectory and subsequent induced fit docking of a set of 14 reference compounds allowed for identification of hERG conformations yielding improved drug−protein contacts. A set of approximately 2000 in-house molecules with known hERG affinity were then used to determine which hERG conformer discriminates best active hERG blockers from inactive molecules.

A comprehensive fuzzy pharmacophore model of typical hERG blockers was derived and compared to previously published pharmacophore models.

Binding orientations of typical hERG blockers are described and discussed. Further evidence is shown in support of previous studies arguing for putative perpendicular binding orientations of hERG blockers.

METHODS

hERG Binding Assay. *Membrane Preparation.* HEK293 cell line stably expressing the human hERG channel was grown at confluence, harvested in PBS buffer (GIBCO, Invitrogen, France) containing 5 mM EDTA and centrifuged at 1000 g for 20 min (4 °C). The resulting pellet was suspended in 50 mM Tris/HCl, pH 7.4, containing 1 mM EDTA, and homogenized using Kinematica polytron. The homogenate was then centrifuged (20 000 g, 30 min, 4 °C), and the resulting pellet was suspended in 50 mM Tris/HCl, pH 7.4, containing 10 mM KCl and 1 mM MgCl2. Determination of protein content was performed according to Bradford, using the Biorad kit (Bio-Rad SA, Ivry-sur-Seine, France). Aliquots of membrane preparations were stored at 80 °C until use.

[^{3}H]-Dofetilide Binding Assay. Dose−responses of compounds were mixed with HEK-hERG membranes (120 fmol/mL) in binding buffer (Tris/HCl 50 mM, pH 7.4, containing 10 mM KCl, 1 mM MgCl2, and 0.1% BSA) in a final volume of 250 L containing [^{3}H]-Dofetilide 5 nM, for competition experiments. After an incubation of60 min at 20 °C, reaction was stopped by rapid filtration through GF/B unifilters coated with 0.1% PEI, followed by three successive washes with ice-cold Tris/HCl 50 mM, pH 7.4 containing 0.1% BSA. Nonspecific binding was defined with 10 μM astemizol. Data were analyzed by using the program PRISM (GraphPad Software Inc., San Diego, CA). Inhibition constants (K_i) were calculated according to the Cheng−Prussof equation: $K_i = IC_{50}/[1 + (L/K_d)]$, where IC_{50} is the inhibitory concentration 50%, L is the measured concentration of [^{3}H]-JLP93, and K_d the dissociation constant of the radioligand. pK_i were calculated as $pK_i = -\log(K_i)$. Experiments were repeated at least 2 times, and compounds with pK_i > 5.3 were flagged as hERG binders.

Homology Modeling. *Pore Domain.* The pore domain of hERG, the most widely studied during the last years using in-silico techniques, corresponds to the central transmembrane part of the channel. Formed by four monomers, it encompasses the selectivity filter but also the currently best characterized drug binding site, right below the selectivity filter. Unfortunately, there is still no 3D-structure available of this particular domain that would allow to derive mechanistic insights on hERG functioning and also the effect of hERG blockers.

However, crystal structures are available now for several other potassium channels. Thus, homology modeling or threading techniques can be considered in order to derive the structure of the hERG pore domain. A plethora of studies exist today, basing themselves on templates like KcsA, MthK, KvAP and lately also Kv1.2/Kv2.1.

As mentioned previously in this manuscript, the hERG potassium channel is known to undergo important conformational changes during a normal functional cycle (transition from active to inactive, active to closed). Considering these conformational states is of importance when deriving binding modes of hERG blockers or hypotheses on functional aspects of hERG. For modeling the hERG channel, only the active state was considered important in order to be able to place small molecules into the known drug binding site. However, we considered the use of two different templates to produce two distinct conformational states, both corresponding to active states. The KvAP structure (PDB code 1orq), in the open state, has been used mainly to be able to produce results comparable to previous contributions. Next we considered the Kv1.2/2.1 chimera (PDB code 2r9r) as most suitable for our modeling work. In contrary to KvAP, the structure of the chimera encompasses the entire transmembrane domain. Thus, also the voltage sensitive domain, which is central for voltage dependent rearrangement of hERG. Throughout this article $M_{Kv1.2}$ refers

dx.doi.org/10.1021/ci5001373 | J. Chem. Inf. Model. 2014, 54, 2320−2333

to the homology model based on the Kv1.2/Kv2.1 chimera, while M_{KvAP} refers to the model based on the KvAP template.

It is noteworthy that despite the fact that both template channels are supposed to be in their active state, significant differences can be observed between both of them. A notable S6 helix bend can be observed on KvAP near the central conduction pore cavity, while the Kv1.2/Kv2.1 lines up straight S6 helices near the pore. This results in a central cavity that is far less solvent exposed in Kv1.2/Kv2.1 compared to KvAP. The sequence alignment used for constructing these homology models are available in Figure S5 in the Supporting Information.

For constructing the homology models, MOE2011.09 has been used. Four distinct chains were modeled using the homology modeling tool available in MOE. Cations present in the conduction pore in the crystal structure were kept during the modeling process. Ten mainchain models with five side chain models have been constructed. All models have been filtered to gather the model with the lowest atom clashes, backbone torsion angle outliers, bond angle outliers. Furthermore, high contact energies between protein residues have been used as criterion to filter out unsuitable homology models.

The finally chosen model was locally refined on areas where unfavorable interactions or atom clashes have been identified.

Molecular Dynamics. Homology models have been subjected to Molecular Dynamics (MD) simulations for further equilibration of the structure given the rather low sequence identity between the available templates and the hERG sequence. The transmembrane tetramer models ($M_{Kv1.2}$ and M_{KvAP}) have been prepared using the protein preparation tool in MOE2011.10, subjected to a minimization under harmonic (Charmm27 force field with a heavy atom tether with force constant of 1) and then exported to a PDB file. This PDB file was then further prepared using VMD.[24] The protein was embedded into a POPC membrane patch surrounded by an aqueous solution of 100 mM KCl.

MD simulations of the apo hERG models were carried out using the program NAMD2.9 (GPU)[25] and the Charmm27 force field for proteins,[26,27] ions[28] and phospholipids,[29] with the TIP3P water model.[30] Periodic boundary conditions were used[31] with constant temperature using Langevin dynamics, maintained at 310 K.

MD Simulations of Docking Poses. For a subset of ligands constrained MD simulations have been performed using NAMD2.9 (GPU)[25] and the Amber99SBildn force field.[32] The environment of the protein (membrane, ions, and water) were taken at the state of the apo MD simulations from which has been extracted the conformation used for induced fit docking. After merging of the protein environment and the protein conformation obtained via Glide Induced Fit Docking[33] all waters overlapping with the binding have been deleted. Next, a solvent analysis of the binding site has been carried out using 3D Rism.[34,35] Water molecules have been placed on the lowest energy spots and hydrogen oriented using Protonate 3D (available in MOE).[36] The potassium residue name was renamed to "K+". Next, two PDB files were written, containing (i) the environment of the protein (water, lipids, ions) and (ii) the protein itself. Furthermore, a mol2 file has been extracted containing parm@frosst atom names in the atom type column instead of Tripos atom types (achieved with a modified version of the file save dialogue). The parm@frosst small molecule parameters have been developed over years at Merck Frosst by C. Bayly, D. McKay and J.F. Truchon and have recently been released to the public. Charge calculations of the ligand have been performed using MOPAC and AM1-BCC charges. Forcefield parameters for the ligand were translated from MOE's parm@frosst parameters to a tleap[37] compatible frcmod file using a SVL script written for that purpose. The GAFFlipid parameters from ref 38 were taken for the lipids and retrieved from lipidbook.[39] Next the full system was constructed using tleap. Importantly, no solvation has been performed by tleap at this stage as all solvent molecules deemed necessary for the simulation are already included in the system.

For all subsequent simulations spherical constraints have been used. The center of that sphere was defined to be 12 Å beneath the S3 potassium site in the selectivity filter along the z axis. All atoms further than 20 Å of that point are fixed, while atoms between 18 and 20 Å distance from that point are set under harmonic constraints. The remaining atoms inside the sphere are kept without any positional constraints.

Next, a short minimization (conjugated gradient) has been performed followed by a gradual heat up to the final temperature (310 K) used throughout the simulation. An equilibration of 0.5 ns was followed by production runs of at least 10 ns.

Accelerated MD Simulation. Accelerated MD was performed starting from a configuration obtained after 40 ns of classical MD on the transmembrane domain of hERG. NAMD 2.9 (GPU) was used to produce a 60 ns production run. For the accelerated MD, only the dihedral potential has been modified in order to allow easier passing of energy barriers. The average dihedral potential was extracted from the previous classical MD simulation (22 250 kcal/mol). For the accelerated MD the Ed has been set to 20 246 400 kcal/mol and alpha to 562.4.

Selection of Reference Snapshots for Molecular Docking. The first 40 ns of the MD trajectory, produced throughout this work, were used to isolate a few snapshots that have been further evaluated for suitability in molecular docking. An all against all RMSD matrix was calculated using only backbone atoms of residues 641−645 and 648−649. This rather unconventional residue selection aimed at isolating conformations of the main cavity that are mainly influenced by residues lined up at the very top of the pocket, situated right beneath the selectivity filter. Key residues like F656 and Y652 have been intentionally discarded from this clustering in order to focus on the upper part of the cavity. Furthermore, the selected snapshots have then been further utilized in induced fit docking, allowing for arrangement of cavity lining residues, including F656 and Y652.

Molecular Docking. Protein−ligand docking was performed using Schrödinger Glide docking program and also Glide Induced Fit Docking (IFD). Geometry optimization calculations for ligands have been carried out using Pipeline Pilot. Molecules were kekulized, standardized charges were calculated, then ionized using the Chemaxon ionizer and last 3D conformations were generated using Corina. The protein was prepared using Maestro and the protein preparation wizard. Glide SP was used together with IFD, and for high throughput docking.

For IFD calculations, side chains were kept and rearranged around a docked pose of the ligand. For conformation (I) of $M_{Kv1.2}$ the following side chains were stripped to allow for bigger adaptations in the symmetrical binding site: F557, F656, M651, Y652. After initial placement of the molecule these side-

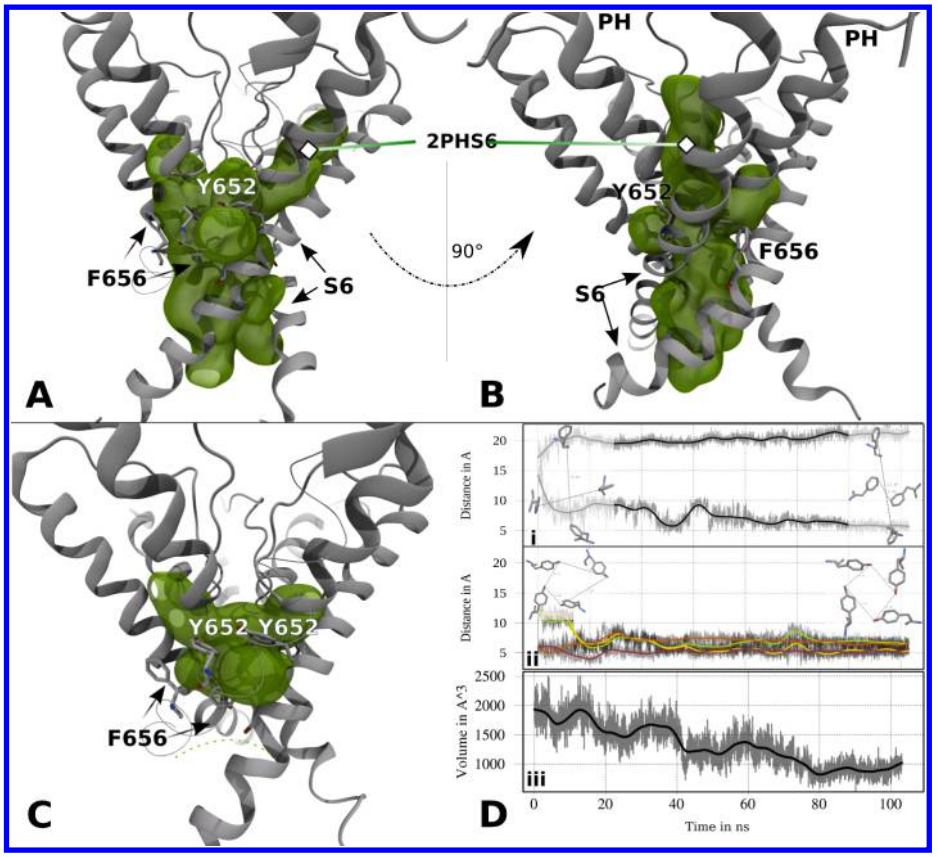

Figure 1. (A) hERG pore binding site during at least 25% of the first 40 ns of the MD trajectory. F656 adopts two distinct conformations. Solvent accessible channels are observed between the S5P, S6, and S5 helices. (B) Same as A but rotated by 90° around the ion transduction axis. (C) hERG pore binding site during at least 25% of the last 65 ns. F656 gate closure yields a much smaller pocket. (Di) Distance between opposing F656 residues during time, (Dii) distance between adjacent hydroxyl oxygens of Y652 during time, (Diii) volume of the pore binding site. **S6**: S6 transmembrane helix. **PH**: pore helix. **2PHS6**: cavity observed between two adjacent pore helices and one S6 helix.

chains have been rebuilt into the binding site and refined by subsequent steps of the IFD protocol.

Pharmacophore Elucidation. In order to isolate characteristic interaction patterns of active compounds we used the in-house data set docked to conformation $(I)_{\text{pimozide}}$. Subsequently, all poses of the most active molecules have been selected ($pK_i > 6$). For each molecule the pose with the best glide lipophilicity score was selected and defined as reference pose. The RMSD versus all other poses of the same ligand was calculated and poses with an RMSD > 1.0 Å from the reference pose were discarded. Next, all remaining poses having a glide lipophilicity score below −6.0 were analyzed to derive a fuzzy ligand based pharmacophore. Hence, this pharmacophore is built up on functional groups and features observed among the most active molecules using only a conserved or best pose.

RESULTS

Shape Dynamics of the Central Cavity and Conduction Pore. In the past decade, research on potassium ion channels discovered the role of two aromatic residues on the conduction pore of the channel. For hERG, these two residues are F652 and Y656. The region surrounded by residues F652 and Y656 below the selectivity filter (indicated on Figure 1A) is known to play a major role in drug induced QT syndrome.[40] Several small molecules are known to bind to this area and much has been speculated about the ability of hERG to recognize a large variety of molecules and structural features allowing it to do so.[41]

Classical and accelerated molecular dynamics simulations were performed on the Kv1.2/2.1 based homology model of hERG in its supposed active state (hereafter referred to as model $M_{Kv1.2}$). These simulations aimed for structure equilibration and at the mean time conformational sampling of the pore cavity for subsequent docking calculations.

During this equilibration the volume of the binding site beneath the selectivity filter has been monitored using MDpocket[42] and VMD.[24] While the cavity appears to be accessible from the cytosol in the beginning of the simulation, the gating residue F656 and global S6 helix movements slowly close the cavity. Figure 1A and B illustrates the state of the cavity at 25% of the time during the first 40 ns of the MD simulation. Illustration C shows the pocket observed at 25% of the time during the last 65 ns of the MD simulation.

Y652 arranges very quickly in a circle around the central cavity. This is shown in Figure 1Dii, highlighting the distance between side chain hydroxyls of the four adjacent Y652 residues. On the contrary and unexpectedly, only two out of four F656 are oriented toward the center of the cavity. This is highlighted in illustration Di, where two opposing phenylalanines (F656) are shown to be in contact during the last part of the trajectory. Previous findings indicate that initiation of cavity closure have been observed in our simulations. This pore closure appears to be linked to transmembrane helix bending events. Bending of two S6 helices is observed throughout the trajectory. This is highlighted on Figure 2, showing the Whisker boxplot of the bending angles observed during the MD

dx.doi.org/10.1021/ci5001373 | J. Chem. Inf. Model. 2014, 54, 2320−2333

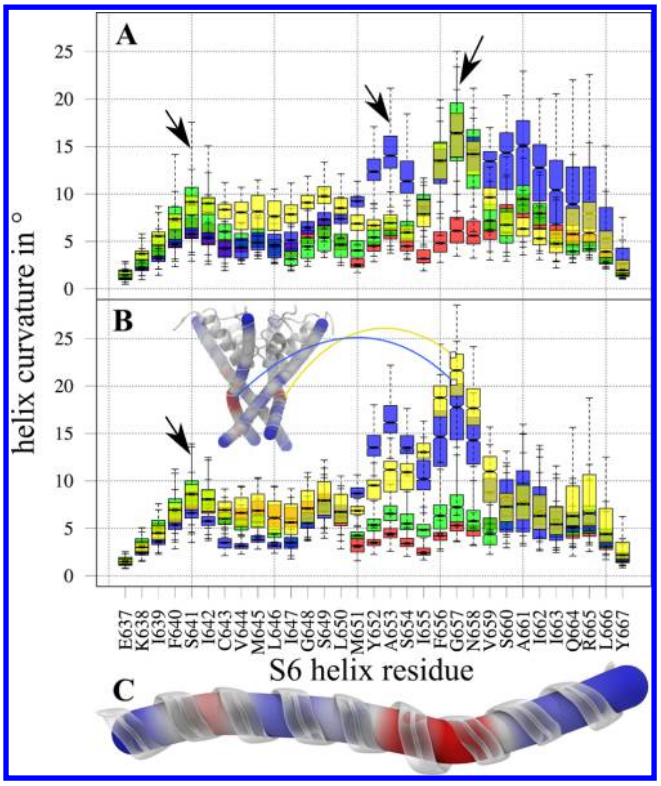

Figure 2. Yellow, red, blue, and green curves correspond to respectively one hERG monomer. (A) S6 helix curvature during the first 40 ns of the MD trajectory. (B) S6 helix curvature during the last 65 ns of the MD trajectory. (C) Example of S6 helix at the end of the trajectory.

trajectory for all residues on helix S6. Each of the four S6 helices is represented by a distinct color (red, green, blue and yellow). Residue G657 is causing S6 to kink in three out of four subunits of hERG during the first 40 ns of the MD trajectory. Interestingly, upon F656 gate closure two out of four S6 helices are straightened (blue and red boxplots on Figure 2B), while the two other opposing helices maintain an important kink on G657. Another helix bend is observed to a lesser extent on A653. Interestingly, the two interacting F656 observed on Figure 1Dii are both situated on the unkinked helices. This result indicates that G657 allows to introduce helix flexibility that permits F656 outward flipping as observed in the end of the trajectory (Figure 2C). It is less clear to which extent A653 contributes to S6 helix arrangement, as curvature in this region could only be clearly observed on a single monomer (Figure 2B—blue boxplot) and to a lesser extent on a second monomer (Figure 2B—yellow boxplot). However, A653 is evolutionary conserved and is known to play a central role in channel closure.[43] The alanine is involved in S6 inter helical packing in a critical region encompassing the F656 gate. The hERG model used in this study is fully consistent with this observation throughout the MD trajectory. Close contacts between the A653 side chain and the adjacent S6 helix can be observed. The moderate ability of the residue to introduce a helix bend might contribute to the possibility to position F656 in the two different configurations observed toward the end of the MD trajectory. Thus, A653 mutations are likely to have a twofold impact on gate closure: (i) S6 helix packing alterations and (ii) perturbations on correct F656 arrangement for gate closure.

A slight helix bend can also be observed on residue S641 (Figure 2). This weak curvature is conserved among all four subunits. Interestingly, S641 has been characterized to be involved in C-type inactivation of hERG. Its replacement by an aspartate or threonine is known to disrupt inactivation, whereas mutants S641A and S641C facilitate C-type inactivation.[44]

S5 helix curvature for all subunits of hERG is shown in Figure S1. Interestingly, two out of four monomers have an important kink at F551. Note that these are the two monomers (red and green) that do not have a kinked S6 helix (Figure 2) and position F656 toward the lumen of the central pore. A further helix bend is observed on the other two monomers further up in the helix around residue L559. Here again both residues have already been described to be critical for hERG activation.[45] F551, L559, and W563 have been described to face toward the voltage sensor domain (VSD).[18,45] This is indeed the case in our hERG model, further contributing to its validation. L559 undergoes direct transient contacts with V532 and V535 situated on helix S4. W563 intermittently approaches V532. However, F551 is situated in an area deprived of putative interactions with the VSD. Thus, with S4 helix down shifted F551 is situated in the lipid bilayer beneath the S4 helix of the VSD. As hERG channel closure involves an important S4 helical shift toward the cytoplasm[11] it is thus very unlikely for F551 to interact in the closed or open state of the channel.

Events Linked to Inactivation. As shown on Figure 1A, the pore binding site appears to encompass a larger area than usually described in literature. This additional accessible area, called 2PHS6 hereafter, is located between two adjacent pore helices and helix S6. Interestingly, similar observations have been made recently by Koepfer and co-workers, also on a Kv1.2 based homology model.[46] 2PHS6 is an area that appears to be transiently solvent accessible.

Koepfer and co-workers assessed the importance of 2PHS6 and residues S620, F627 and N629 for hERG inactivation. Importantly, it is hERG C-type inactivation that impacts the QT-interval. The authors found that direct hydrogen bonding of N629 to S620 induces a collapsed state of the selectivity filter of hERG. Mutations of either of these residues or residues nearby have a direct effect on C-type inactivation of hERG.

Interestingly, several similar observations can be made from our MD simulations. Figure 3 shows a detailed view of the residues situated behind the selectivity filter on one hERG monomer. Although N629 was initially situated between 6 and 8 Å a part from S620, several spontaneous direct hydrogen bonds have been observed in the beginning of the MD simulation. Such a direct H bonding state is shown on Figure 3. The hydrogen bond network behind S620 is also shown on the figure and displays a very well conserved connection linking S620 to Y616 of an adjacent hERG subunit. The importance of the hydrogen bonding network as shown here has also been highlighted by Koepfer et al. and investigated using a Y616F mutant. Upon mutation of the tyrosine to the hydroxyls missing phenylalanine a strong inward rectification was observed by the authors. Given the H-bond network observed during our MD simulations the role of S641 and S621 could appear equally important. Previous studies have also shown that S641 mutations impact hERG inactivation[44] and S621 implications in activation, deactivation and inactivation have been investigated by Lees-Miller and co-workers.[47]

A substantial difference between the work presented here and simulations performed by Koepfer et al. is that the distance between N629 and S620 evolved freely during the MD in our

dx.doi.org/10.1021/ci5001373 | J. Chem. Inf. Model. 2014, 54, 2320−2333

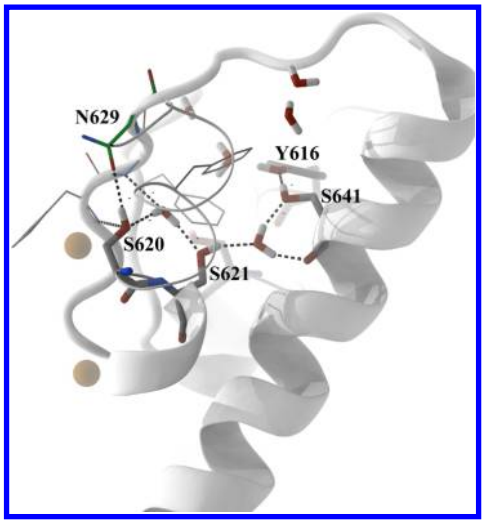

Figure 3. Hydrogen bond network observed behind the selectivity filter, between residues N629, S620, Y616, S621, and S641.

simulations. Furthermore, the selectivity filter remained structured with two potassium ions steadily occupying the filter. Thus, collapse of the selectivity filter has not been observed. However, similar to Koepfer et al. we observed also a V625 backbone carbonyl flip in the beginning of our simulation (red curve in Figure S2).

Toward Novel Binding Hypotheses for hERG Blockers. A multitude of articles have been published on the putative positioning of hERG blockers.[12,14,20,48−50] Despite thorough investigation no consensus on binding modes of known blockers has emerged yet. Historically, homology models of hERG have been used together with mutagenesis data to spot the binding site of drugs,[3] but only lately the high plasticity of the binding site has been taken into account to rationalize positioning of small molecules.[20] Furthermore, several papers have been published during the last years highlighting other binding sites in the pore domain. These could also potentially accommodate hERG activators and blockers.[46,51] Given the plasticity of the pore domain, we deem it important to thoroughly analyze transiently accessible space in the pore domain of the ion channel.

Extraction of Protein Conformations on the Kv1.2 Based hERG Model. The previously described MD trajectory was also used to extract 6 representative snapshots of the first 40 ns of the trajectory obtained on $M_{Kv1.2}$. These have been derived using hierarchical clustering (centroid linkage) based on the backbone RMSD of the pore domain calculating a distance matrix of all snapshots versus all snapshots.

We selected 14 reference ligands (Supporting Information Table S2) with measured hERG binding activities in competition with dofetilide as radioligand. Induced Fit Docking (IFD) was performed for these ligands on all six protein conformations isolated previously. The Glide SP docking score was used to detect putative discrimination between high affinity binders and known nonbinders by analyzing the top *N* poses, where *N* varied from 1 to 10. Here IFD methodologies were used to consider explicitly the plasticity of the central cavity of hERG.

Using IFD, two conformations have been isolated, numbered (*I*) to (*II*). Conformation (*I*) yielded the most promising results. Performance was measured by the ability of the docking score to differentiate hERG binders from non binders in this set of 14 reference ligands (results not shown). For each of these conformations the top scoring pose of one or two top scoring ligands have been used to extract the final induced fit conformation of the channel for further use. This resulted in hERG conformations $(I)_{astemizole}$, $(I)_{fluspirilene}$, and $(II)_{astemizole}$. To enhance the number of interesting IFD derived protein conformations for high-throughput docking, another conformation was derived using a different IFD protocol on (*I*). Here side chains were stripped prior to initial ligand placement and afterward rebuilt and refined around the ligand. An interesting conformation was obtained by docking pimozide and named $(I)_{pimozide}$ hereafter. Thus, in total four conformations of interest have been retained for further analysis.

Extraction of Protein Conformations on a KvAP Based hERG Model. The second hERG model, derived using a KvAP X-ray crystal structure (M_{KvAP}) as template has also been subjected to a MD simulation. Hierarchical clustering (centroid linkage) based on the RMSD of the pore domain was undertaken. The most representative snapshots of the resulting clusters where retained, resulting in six different conformations named (*A*) to (*F*). Given the fact that all of these conformations contain a very open central cavity, they have been selected directly for subsequent high-throughput docking studies.

Table 1. Early and Global Enrichment Performance Indicators for Docking 1387 Molecules (1096 Inactive and 291 Actives) to Different Protein Conformations[a]

	Glide docking score					Glide lipophilicity score				
conformation	EF_1	EF_5	AUC	BR_5	BR_{20}	EF_1	EF_5	AUC	BR_5	BR_{20}
$(I)_{astemizole}$	2.09	2.16	0.71	0.52	0.43	3.05	2.79	0.86	0.71	0.62
$(I)_{fluspirilene}$	0.69	1.39	0.68	0.45	0.30	3.39	3.25	0.84	0.69	0.63
$(I)_{pimozide}$	3.93	2.81	0.78	0.62	0.58	**4.73**	**4.42**	**0.89**	**0.80**	**0.80**
$(II)_{astemizole}$	3.40	3.53	0.74	0.60	0.64	3.40	3.60	0.88	0.77	0.74
(*A*)	3.03	3.03	0.73	0.57	0.56	4.40	3.99	0.87	0.77	0.78
(*B*)	3.78	2.47	0.73	0.57	0.53	**4.41**	**4.34**	**0.88**	**0.78**	**0.80**
(*C*)	2.75	3.10	0.77	0.62	0.60	4.75	4.00	0.90	0.78	0.78
(*D*)	4.41	3.24	0.77	0.61	0.61	4.41	3.99	0.87	0.75	0.76
(*E*)	1.72	2.34	0.71	0.55	0.50	4.06	4.06	0.87	0.76	0.77
(*F*)	3.37	2.96	0.76	0.62	0.59	4.06	3.72	0.88	0.77	0.75

[a] EF_x: enrichment factor at *x*%. AUC: area under the receiver operator characteristic curve. BR_x: BEDROC[54] early enrichment measure at α of 5 and 20.

dx.doi.org/10.1021/ci5001373 | J. Chem. Inf. Model. 2014, 54, 2320−2333

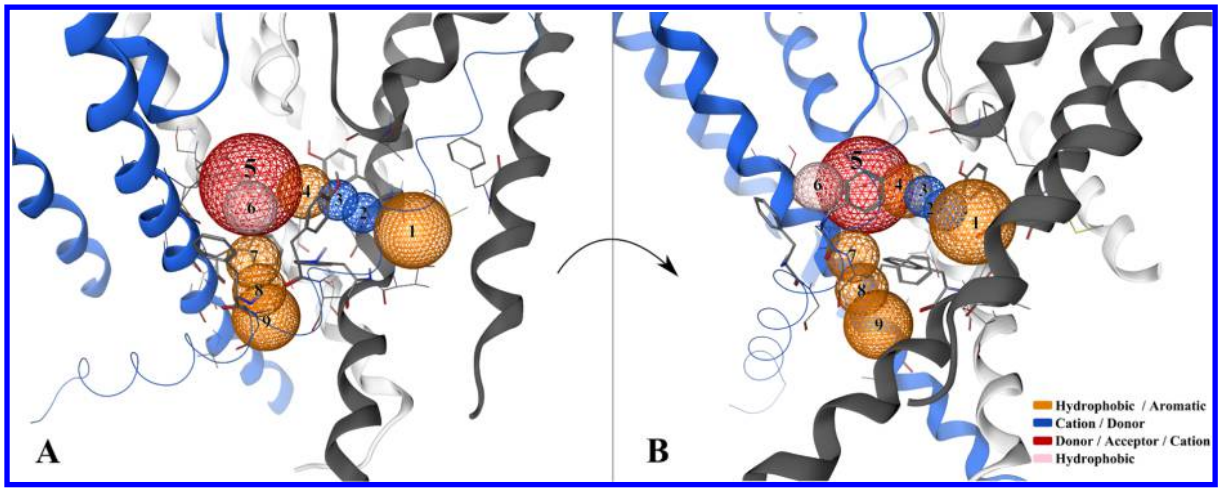

Figure 4. Fuzzy pharmacophore derived from most active ligands ($pK_i > 6$) and best poses glide lipophilic score <−6.0. (A) View of the central cavity. (B) Same as A, slightly rotated around the z axis (conduction pore). **1**: Hydrophobic or aromatic area in the backpocket toward F557. **2**: Putative cation or donor placement in contact with backbone carbonyl of Y652. **3**: Putative cation or donor placement in contact with side chain hydroxyls of Y652. **4**: Hydrophopic or aromatic area. **5**: Polar area below the selectivity filter was found to fit donors, acceptors and positive charges. **6**: Hydrophobic area next to Y652 and F656. **7**−**9**: Hydrophobic/aromatic areas lining F656 and helix S6 of the adjacent subunit of the channel.

High Throughput Docking into hERG Conformations. All previously described conformations obtained from $M_{Kv1.2}$ and M_{KvAP} have been used for screening an in-house library of 1969 small molecules with known binding affinity to hERG. This library was composed of 1096 inactive molecules ($pK_i < 5$), 291 active molecules ($pK_i \geq 6$) and 582 moderately active molecules ($5 \leq pK_i \leq 6$). After docking each compound into each hERG conformation using Glide SP,[52] only the top five poses per protein conformation were retained (ordered by either the glide docking score or glide lipophilicity score). An average docking score (glide docking score or glide lipophilicity score) of these five poses was calculated and subsequently used for ranking the compounds. Table 1 summarizes various performance indicators for enriching the results in active hERG molecules. In the subsequent section only the classification between active and inactive molecules has been analyzed. Overall, a relatively modest prediction performance is observed for all protein conformations if the average glide docking score (SP) is used to rank the molecules. Using the glide docking score, mainly conformations $(I)_{pimozide}$ and (D) perform best. Interestingly, prediction performance appears to be improved when using the averaged glide lipophilicity score for ranking compounds. Results are globally better than ranking based on the glide docking score. Another interesting observation is that nearly all conformations based on the very open central cavity (KvAP based homology model) yield relatively high prediction performance, while conformations (I) to (II) appear to be more stringent. Nevertheless, conformation $(I)_{pimozide}$ turned out to be the most predictive among all conformations analyzed throughout this work.

Another interesting fact is that scoring and ranking using a lipophilicity based score yields more encouraging results than using the glide docking score. This is in line with various observations that hydrophobic contacts are central for hERG activity,[53] while cation−π interactions might have been overestimated in the past. Calculation of average docking scores has also been performed using 1, 3, and 10 poses instead of 5, without significant performance improvements (data not shown).

Given the high plasticity of the hERG binding site a ligand could potentially bind equally well into different conformational states of the channel. To answer that question the best binding poses of sertindole were analyzed on all hERG conformations considered in this analysis. The recorded pK_i value for sertindole is 6.9 and thus the molecule can be considered as moderately to weakly active. Such moderate hERG activities can typically hinder the progression of a molecule during lead optimization stages.

When analyzing the rank of the best binding pose of sertindole one can observe that it is systematically ranked among the 15 to 24% of best scored molecules. Only for the conformation $(I)_{astemizole}$ it is ranked within the top 2%. This high ranking on this particular conformation appears to be reasonable given the high similarity between astemizole and sertindole. In three out of the closed conformations of hERG considered here, the best pose of sertindole has been found within the top 15−17% of all ligands, while in five out of six open conformations the best pose was found within the top 21−24%. The closed conformation appears to allow a slightly better ranking of sertindole binding poses compared to the open hERG conformations.

Deriving Frequently Occurring Interaction Patterns. The previously obtained docking results were then used to derive frequently occurring interactions. Three different locations can be clearly identified. Polar or cation placement positions are observed beneath and next to the selectivity filter. This result is at odds with earlier works that often proposed positioning of the typical tertiary amine at the level of F656 in order to undergo cation-π interactions with the phenyl ring. However, according to literature cation-π interactions are less often observed with phenylalanines compared to tyrosines or tryptophans.[55,56] This corroborates with results presented in this study. Figure 4 schematically illustrates positioning of the most active molecules from the in-house data set. This simplified representation allows to describe parts of the feature contributing to the activity of these hERG binders. The most conserved features are aromatic and hydrophobic moieties in areas 1, 7, 8, and 9. Areas 7, 8, and 9 already have been described in previous contributions on placement of hERG

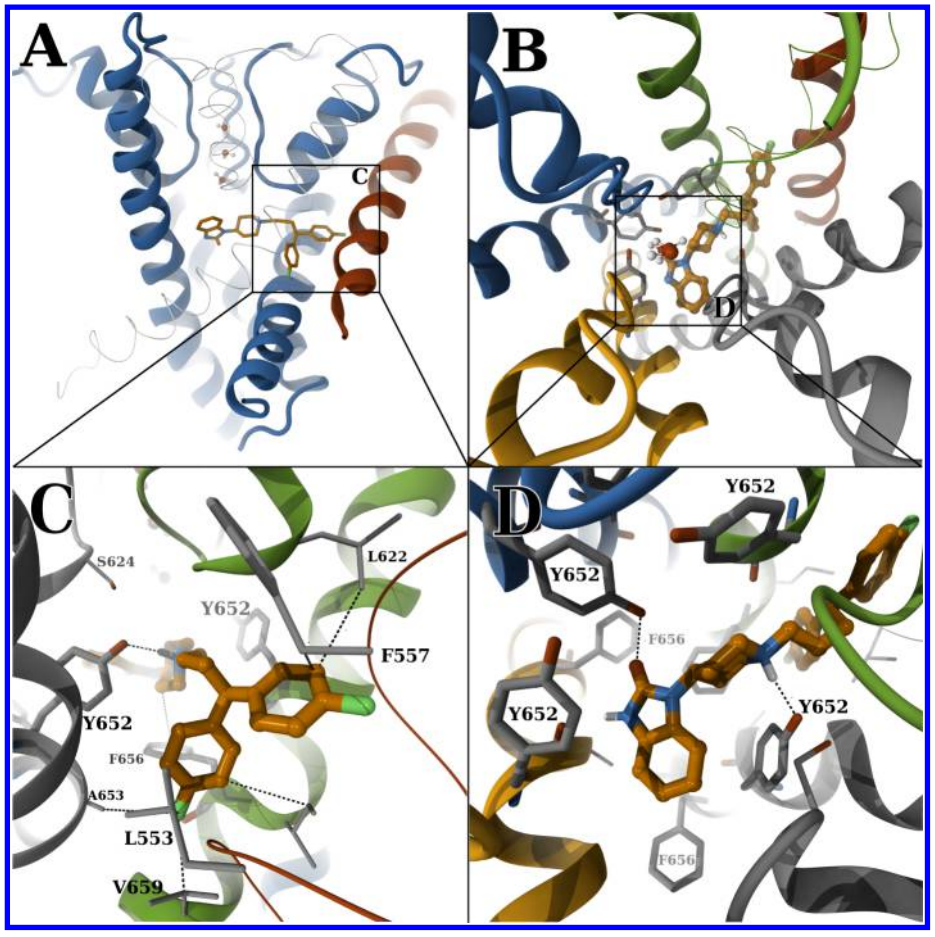

Figure 5. Pimozide placement obtained with Glide IFD resulting in conformation $(I)_{\text{pimozide}}$. (A) Side view. (B) Top view. (C) Detailed view of hydrophobic interactions in a side pocket opened beneath mainly via Y652 rearrangements beneath a S5P helix. (D) Detailed top view of zone beneath the selectivity filter.

blockers, whereas area 1 has been made accessible by docking pimozide under induced fit. Here we clearly identified two aromatic hotspots, underlining the importance of hydrophobicity in hERG blockers. Next, a rather conserved area of putative positive charges or hydrogen bond donors was observed in area 3, allowing to interact with the hydroxyls of Y652 or undergoing cation−π interactions with Y652. Area 4 can also be considered as being able to accommodate for positive charges or hydrogen bond donors. In areas 3 and 4 other moieties have also been observed, but only the most prominent have been highlighted in this analysis. Both of these areas are also exclusive, meaning that if a donor or charge is located in 3 it is unlikely to find another donor or charge in area 4 and vice versa. Unexpectedly, a small hydrophobic zone was observed in area 6. Its presence is likely due to the neighboring F656 and Y652. Area 5 is defined to encompass a major part of the zone right beneath the selectivity filter. This area contacts residues like S624, as well as transduced water or potassium ions in the filter itself. For this particular area no clear consensus has been observed, but a rather large variety of possibilities to place polar moieties. Thus, area 5 is likely to be able to host various types of interaction partners, including tertiary amines, a hallmark of hERG blockers.

In summary, three locations for putative placement of positively charged moieties are observed. These areas are flanked by hydrophobic and aromatic interaction hotspots. A distance matrix of the identified areas is provided as Supporting Information (Table S1).

Solvation Analysis. Much has been speculated about the importance of tertiary amines for hERG activity. Early modeling works of the hERG channel placed small molecules in-line with the ion transduction axis. Such placements often resulted in placing tertiary amines in contact with F656, supposing cation−π interactions between the two partners.[48] During the last years several studies started to suggest that (i) the interactions with the tertiary amines are not that important to activity[53] and (ii) that they could also be placed in other locations in the central cavity.[48] In light of the previously obtained results on docking compounds to conformation $(I)_{\text{pimozide}}$, our results also do suggest alternative amine placements.

Subsequently we analyzed solvation patterns of the central cavity using conformation $(I)_{\text{pimozide}}$ and 3D-Rism[34,35] exposed via MOE. Figure 6 shows results obtained for positive and hydrophobic probes. For the sake of comparison, the viewpoint of the image is identical to Figure 5A. The hydrophobic isosurface in 1 and 2 overlap very well with the diphenyl moeity of pimozide (Figure 6D). Another hydrophobic area is observed (3) toward the bottom of the cavity. This area corresponds indeed to a pinch in the cavity formed by two out of four F656 residues (cavity shape shown on figure S4).

The blue isosurface (Figure 6a−d) shows regions that are accessible for positively charged probes. Region a in Figure 6

dx.doi.org/10.1021/ci5001373 | J. Chem. Inf. Model. 2014, 54, 2320−2333

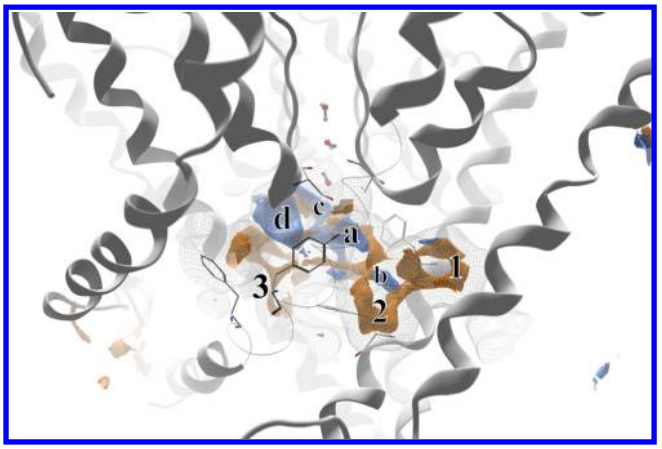

Figure 6. Isosurface maps of 3D-Rism derived interaction energies of (**blue**) positive probes at isolevel 4 and (**orange**) hydrophobic probes at isolevel 4. Areas 1−3 are assigned to hydrophobic zones, while a−d are assigned to areas where positive charges could be placed.

corresponds to the location where the tertiary amine of pimozide is placed. Not surprisingly several other locations are found in the environment. Region c corresponds to the area beneath the selectivity filter. Region d is situated right next to the backbone carbonyl of T623, beneath the selectivty filter. The carbonyl is very solvent accessible and according to 3D Rism calculations a higher desolvation penalty is involved if water is to be replaced. Smaller, but nonetheless interesting is region b. It is situated on the opposite side of area a in the same horizontal subpocket. Here a putative interaction of positive probes and the backbone carbonyl of Y652 is suggested, allowing compounds to orient i.e. tertiary amines toward the side chain hydroxyls of Y652 or the backbone carbonyl of Y652 on an adjacent hERG subunit.

These results suggest that several areas around the base of the selectivity filter could potentially act as interaction partner for positively charged probes. Furthermore, a horizontal subpocket (versus the vertical ion transduction axis) provides further putative interaction spots. Areas a−d encompass a rather large zone which could allow hERG to adapt to a large variety of tertiary amine or hydrogen bond donor containing hydrophobic compounds.

When comparing results obtained with 3D-Rism and results previously exposed as fuzzy pharmacophore, several parallels can be observed. Aromatic/hydrophobic areas match well and also areas a and b from Figure 6 are found in regions 2 and 3 in the fuzzy pharmacophore (Figure 4).

In completely independent simulations of a hERG model based on the KvAP structure (1orq), the protein was simulated under harmonic constraints in the presence of solvent mixtures composed of 20% ethanol/80% water or 20% acetamide/80% water. Despite harmonic constraints of the model, strong ethanol binding was observed in the regions of interest here, encompassing mainly Y652 and T623. While no spontaneous opening toward F557 has been observed these results clearly suggest that hydrophobic moieties could potentially bind there.

Comparison with Reference Pharmacophore Models. Purely ligand based approaches have been used for a decade to describe and predict the activity of hERG blockers. Due to unavailability of the 3D structure of the channel, QSAR and pharmacophore models provided first insights into common features on small molecules able to impair proper hERG functioning. Here we compare the results exposed in previous paragraphs with a consensus of these models frequently found in literature.

Cavalli and co-workers published an initial pharmacophore model in 2002.[6] This work presented a 3D CoMFA based model of hERG blockers as a triangle of hydrophobic/aromatic features with a central positively charged nitrogen. See Figure 1b and Table 2 in ref 6 for detailed geometry. The authors observed a distance of 4.3−6.7 Å between the two first hydrophobic/aromatic features (C0−C1 in the paper). Given results obtained in our study, it is very likely that both features C0 and C1 from ref 6 correspond to the area where the diphenyl has been placed in conformation $(I)_{\text{pimozide}}$, shown in Figure 5D. In fact the distance between the center of both phenyl rings is measured to be about 4.9 Å in the IFD binding pose of pimozide which was retained previously. This corresponds to the interval given by Cavalli et al. In the fuzzy pharmacophore shown in Figure 4 this particular area is encompassed in zone 1.

Next, the 2002 pharmacophore model proposed a basic nitrogen to be situated between 5.2 and 9.1 Å from the first of these hydrophobic/aromatic areas, and 5.7−7.3 Å from the second. Here again the result is in good agreement with results observed in solvation analysis and the fuzzy pharmacophore derived from high throughput docking, where the distance from the diphenyl rings of pimozide to the pharmacophore 3 is about 5 and 6.6 Å, respectively. The high variability of these distances also indicate that the position of the basic nitrogen is not necessarily always restrained to be in area 2 or 3 (cf Figure 4; a or b cf Figure 6) but can also be found in adjacent areas 5 (Figure 4 and c/d Figure 6), as previously shown in the fuzzy pharmacophore. Simplified pharmacophore models, as proposed by Cavalli et al,[6] have been subsequently refined by Kramer and co-workers.[17]

Charged tertiary nitrogens are clearly a hallmark of active hERG compounds. Nevertheless, also neutral molecules are found to be active on hERG to some extent. Aronov focused on such compound series, proposing alternative pharmacophore models.[10,57] Interestingly, this alternative pharmacophore also matches to a certain extent the fuzzy pharmacophore proposed here. The hydrophobic triad could be formed by areas 4, 6, and

Table 2. Early and Global Enrichment Performance Indicators for Docking 368 Molecules to Two Different hERG Conformations[a]

	Glide docking score					Glide lipophilicity score				
conformation	EF_1	EF_5	AUC	BR_5	BR_{20}	EF_1	EF_5	AUC	BR_5	BR_{20}
$(I)_{\text{pimozide}}$	2.17	3.11	0.83	0.77	0.82	3.54	2.61	0.78	0.63	0.68
(B)	1.61	2.84	0.76	0.62	0.65	2.04	1.63	0.79	0.61	0.50

[a] EF_x: enrichment factor at x%. AUC: area under the receiver operator characteristic curve. BR_x: BEDROC[54] early enrichment measure at α of 5 and 20.

dx.doi.org/10.1021/ci5001373 | J. Chem. Inf. Model. 2014, 54, 2320−2333

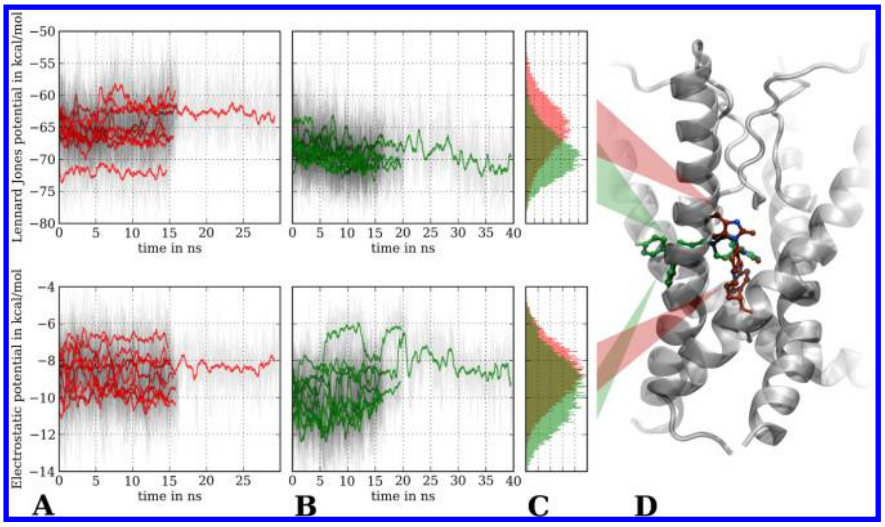

Figure 7. Interaction energies (Lennard-Jones and electrostatics) between pimozide and hERG in (**green**) the horizontal pose retained in this study, (**red**) a vertical pose often assumed in literature.[15] (A) Interaction energies of 10 replicas of the vertical pose. (B) Interaction energies of 10 replicas of the horizontal pose. (C) Distribution of energies between the two poses. (D) Overview of the system with the two poses analyzed here.

7, while acceptors A1 and A2 from ref 10 are likely to correspond to area 5 right beneath the selectivity filter.

Comparison with Public Data Sets. In 2011, Marchese-Robinson and co-workers published a ligand based hERG activity modeling work highlighting several literature data sets, notably the Thai-313 and Dubus-203 data sets.[58,59] In the same work the authors introduced a novel data set, subsequently named Marchese-368.[5] This set was composed of 79 active and 289 inactive molecules. We subsequently evaluated previously identified protein conformations on docking compounds from the Marchese-368 data set. Here we used directly the binary classification established by the authors, despite the fact that medium active compounds ($5 < pIC_{50} < 6$) were included into the inactive class of molecules. Table 2 resumes results obtained on the two previously selected protein conformations, $(I)_{pimozide}$ and (B).

The overall prediction performance appears to be lower compared to the previous analysis on our in-house data set. This result is expected as the data set contains data of active, inactive and moderately active molecules. Moreover the data was obtained from different literature sources making it likely that experimental procedures differ slightly among the same data set. Nevertheless, moderate enrichment can be observed for both conformations. Especially conformation $(I)_{pimozide}$ yields acceptable early and overall enrichment (EF5 and AUC) using the glide docking score and good early enrichment using the glide lipophilicity score. More interestingly, these results clearly highlight the fact that using very open channel templates for homology modeling appears to be counter-productive if then further used for molecular docking. Here the results clearly show that the $(I)_{pimozide}$ conformation has a clearly higher predictive power compared to the very open hERG conformation (B).

Horizontal versus Vertical Binding of Pimozide. In this article we investigated two different binding modes of the potent hERG inhibitor pimozide. First we considered a longitudinal binding mode (in $M_{Kv1.2}$), reproducing several of the earlier works on placement of hERG inhibitors. Here the benzimidazolinone is placed beneath the selectivity filter and the basic nitrogen is placed to form cation π interactions with F656. Second we considered the pimozide binding mode obtained via MD and IFD calculations (hERG conformation $(I)_{pimozide}$). Both binding modes were subjected to short MD simulations (10 replicas 15 ns each) under spherical constraints. Figure 7 shows the Lennard-Jones (6−12) potential (top) and the Coulomb potential (bottom) of the interaction between pimozide and hERG. Results for all replicas are overlaid on the same plot and energy histograms are shown on Figure 7C. The green curves correspond to results obtained on the horizontal binding pose (green pose on Figure 7D), while the red curves show results for the longitudinal binding pose (red pose on Figure 7D). The Lennard-Jones potential for the horizontal binding pose appears to be more favorable than for the vertical biding pose. This difference is less obvious for the Coulomb potential, but here again the potential appears to be slightly in favor of the horizontal binding pose. These results clearly corroborate that high affinity binding to hERG could implicate other than vertical binding modes and that high-throughput docking on conformation $(I)_{pimozide}$ yielded better results than on conformation (B). Hence, these results are clearly in line with observations made by Zachariae and Garg[49,60] in two independent studies.

Influence of the Binding Mode on Inactivation. Very strong parallels were found between the horizontal pimozide binding mode investigated here and 3-nitro-*n*-(4-phenoxyphenyl) benzamide (ICA-105574) from ref 60. ICA-105574 is a compound that has been discovered to shorten the duration of cardiac action potentials by modulating the voltage dependence of hERG inactivation. In the contribution by Garg and colleagues[60] the authors show that ICA-105574 is able to attenuate hERG inactivation, but also enhance inactivation of a closely related channel, EAG. The authors found that ICA-105574 binds to the same binding site in both proteins. Only differences in mechanisms of inactivation gating determine the specific effect for each channel.

Interestingly, the horizontal binding mode of pimozide in conformation $(I)_{pimozide}$ is in contact with all residues that have been identified by Garg and coauthors to be of importance for binding ICA-105574 (see Figure 5C for more information). This result suggests, that also hERG blockers could potentially occupy the binding site first described by Garg and co-workers. This assumption appears to be reasonable given that the

dx.doi.org/10.1021/ci5001373 | J. Chem. Inf. Model. 2014, 54, 2320−2333

authors were able to convert a ICA-105574 from a hERG activator to a hERG blocker simply by mutating A653 to a methionine.

DISCUSSION

More than ten years ago studying the characteristics of small molecules impairing proper hERG functioning became of interest to pharmaceutical industry. Today, experimental testing of novel compounds for hERG activity is standard procedure in modern drug discovery processes. Despite this fact, concepts of hERG blocking by small molecules are still poorly characterized or understood. This hinders establishing rational synthesis rules for medicinal chemists to lower hERG activity of compounds of interest.

Given the structural complexity of ion channels and issues of crystallizing transmembrane proteins, still very few structural information on related ion channels is available. For this reason mainly ligand-based approaches have been used in the past to derive first characteristics of hERG blockers.

Nevertheless several structure-based studies have been published during the last years. Generally, one of the few available crystal structures of remotely related ion channels is chosen as template to build homology models of hERG. Within this article we have shown that the choice of this template is of utmost importance for further molecular modeling work.

Choice of the Template and the Conformation. Historically, structure based modeling of hERG has been undertaken using KvAP, KcsA or MthK crystal structures as templates for homology modeling work, as these were the first ion channels to be crystallized. All of these channels have important differences when compared to hERG and non of them corresponds to a channel found in a closely related species to *Homo sapiens*. Another important issue when modeling ion channels is their inherent flexibility. Thus, ideally, one has to consider several conformational states of the channel for subsequent modeling work. In the work presented in this paper a homology model based on the only mammal ion channel yet crystallized (Kv1.2/2.1 chimera) was built. Another model of hERG was built, this time choosing KvAP (PDB code 1orq) as template, a very often used template in structure based modeling work. Results on subsequent molecular docking suggest that modeling a completely open state of the hERG channel hinders sound explanations of high affinity binding of hERG blockers to the central cavity. Very open conformations of the hERG channel was found to be less useful for identification of potential hERG binders using high-throughput docking techniques. Thus, in upcoming works on positioning and docking small molecules to hERG channel models, considering narrower central cavities should be considered.

hERG Closure Dynamics. The work presented in this paper shed new light on unique features of hERG closure dynamics. Interestingly, hERG monomer pairwise closure movements have been observed. S6 helical bending events appeared to be specific to two helices facing each other, while the other two adjacent helices followed proper bending dynamics. This difference in dynamical behavior is explained by a differential placement of F656 on the two adjacent S6 helices. While Y652 arranges in a circle upon channel closure, F656 of two facing helices is placed toward the lumen of the conduction pore and the two other F656 residues lining the conduction pore. This closure behavior has not been described until now and its functional role is yet to be clarified.

Modeling Techniques and Dependence on Actual Binding Mode. Interestingly, relatively good concordance has been found between previous ligand-based studies of hERG blockers and the high-throughput docking carried out within this study. Results reported in this article allowed to corroborate previously published characteristics of hERG blockers derived using ligand based techniques with structure based results from homology modeling, molecular dynamics and high throughput docking simulations. The structurally derived fuzzy pharmacophore model presented in this work is in good agreement with previous ligand-based pharmacophore models of known hERG blockers.

Positioning of hERG Blockers into the Central Cavity. Various studies intended to propose and validate binding modes of known hERG blockers. Today, there is still no consensus on the binding mode of known hERG blockers. One can roughly distinguish three different ways of positioning hERG blockers into the central cavity: (i) the blocker is oriented vertically vs the transduction axis,[50] (ii) the blocker is oriented horizontally lining the cavity,[48] (iii) the blockers is oriented horizontally penetrating toward the membrane or helix S5.[49,60]

Historically, hERG blockers were thought to bind vertically to the central cavity and hence several contributions proposed such binding modes,[12,15] but also more recent contributions lined up evidence for such binding modes for different types of hERG blockers.[22,50]

In 2005 Farid and co-workers provided insights into novel putative hERG blocker placements, modeling a widely open central cavity of hERG based on a KvAP crystal structure. Using induced fit docking techniques[33] and interaction potential mapping, the authors proposed binding modes lining previously known key residues as Y652 or F656 but placing the molecules horizontally compared to the ion transduction axis. The authors established the following list of observations on interactions of known hERG blockers (sertindole analogues, cisapride, terfenadine, MK-499, ...): (i) extensive ring stacking or hydrophobic interactions with Y652 and F656, (ii) polar groups (and basic centers) can interact with S624 or nearby polar backbone atoms, (iii) able to form hydrogen bonds with polar side chains or backbone atoms, (iv) attraction of a basic center by the negative field within the pore. These results were clearly at odds with previous findings suggesting vertical placement of hERG blockers driven by cation π interactions between the basic nitrogen and F656. Another hallmark of the binding modes proposed by Farid and co-workers was that large molecules would coat the inner cavity surface in the cavity lumen. In other words, the ligands do not penetrate between helices S5 or S6, but rather place themselves in a circular manner to allow a horizontal binding mode versus the transduction pore.

In 2009, Zachariae and co-workers proposed a novel binding mode of typical hERG blockers.[49] This binding mode considered placement of the drug inside the central cavity that is also perpendicular to the pore axis. The cavity basis was formed by Y652 in its pore facing conformation and the authors argued that this conformation can be especially found in inactivated hERG. The authors furthermore explain that longitudinal binding is unable to explain high affinity binding of some well-known hERG blockers. Last, C-type inactivation is suggested to be linked to high affinity drug binding and the flexibility of Y652.

Garg and colleagues proposed a slightly different binding mode compared to the one obtained by Zachariae et al.[60] In this work, the authors present mutagenesis data for hERG and the effect of these mutations on binding known hERG activators. The authors identified a series of amino acids to play a critical role for binding hERG activators: L622, F557, Y652. More intriguingly, the mutation A653M switched an activator to an inhibitor. Interestingly, all residues implicated in binding the activators imply a horizontal binding mode beneath the selectivity filter. This has further been highlighted by the authors in subsequent molecular modeling work. Importantly, there appears to be a very sensitive switch between agonist or antagonist activity.

Results presented in this paper also suggest that hERG blockers can bind horizontally compared to the transduction axis. By docking pimozide using induced fit docking and subsequent molecular dynamics more favorable interaction energies have been observed. Especially shape complementarity (van der Waals potential) was greatly improved when the ligand was placed horizontally and into a more closed conformation of hERG.

hERG blockers encompass a large variety of molecules. They range from small molecules of relatively low weight to large molecules with a variety of ramifications. It is thus very likely that the flexible Y652 and F656 can adopt a variety of conformations. Within this work pimozide has been shown to be able to enter into horizontal subpockets below the selectivity filter. This positioning allowed contacts with the otherwise distant S5 helix. While this subpocket was opened during IFD of pimozide others on the symmetric subunits remained closed. Thus, the overall positioning proposed is yet nonsymmetric on the protein structure. It is however very likely that the highl y symmetric topology of hERG allows opening of such lateral subpockets toward S5 on other subunits. Such openings would allow binding of rather large symmetrical (or nearly symmetrical) molecules in a horizontal binding mode, rather than the classical vertical binding mode.

■ ASSOCIATED CONTENT

Supporting Information

Detailed information on the pharmacophore of frequent interaction patterns of hERG blockers with the channel. The detailed list of reference ligands used in this study is shown. Figure S1 shows helix S5 curvature statistics obtained during the MD trajectory studied in this work, and Figure S2 details torsion angles observed on V625 for all four hERG subunits during the MD trajectory. The Ramachandran plot of the MD trajectory is shown in Figure S3, and the binding pose of pimozide inside the channel is represented on figure S4. The sequence alignment used for the homology model building is represented in Figure S5. The video published as supporting information shows the hERG closure motion obtained using molecular dynamics described within this paper. The zipped file contains six snapshot structures of the molecular dynamic simulation. These six structures have been selected by clustering the first 40 ns of the simulation as described in the paper. This material is available free of charge via the Internet at http://pubs.acs.org/.

■ AUTHOR INFORMATION

Corresponding Author

*E-mail: pierre.ducrot@fr.netgrs.com.

Notes

The authors declare no competing financial interest.

■ ACKNOWLEDGMENTS

The authors thank Olivier Nosjean, William Cohen, and Adeline Giganti for providing in-house experimental binding assay and patch clamp results as well as Charles Tordjman for instructive discussions.

■ REFERENCES

(1) Roden, D. M.; Viswanathan, P. C. Genetics of Acquired Long QT Syndrome. *J. Clin. Invest.* **2005**, *115*, 2025−2032.
(2) Roden, D. M. Drug-Induced Prolongation of the QT Interval. *N. Engl. J. Med.* **2004**, *350*, 1013−1022.
(3) Vandenberg, J. I.; Perry, M. D.; Perrin, M. J.; Mann, S. A.; Ke, Y.; Hill, A. P. hERG K+ Channels: Structure, Function, and Clinical Significance. *Physiol. Rev.* **2012**, *92*, 1393−1478.
(4) Potet, F.; et al. Identification and Characterization of a Compound That Protects Cardiac Tissue from Human Ether-a-Go-Go-Related Gene (HERG)-Related, Drug-Induced Arrhythmias. *J. Biol. Chem.* **2012**, *287*, 39613−39625.
(5) Marchese-Robinson, R. L.; Glen, R. C.; Mitchell, J. B. O. Development and Comparison of hERG Blocker Classifiers: Assessment on Different Datasets Yields Markedly Different Results. *Mol. Inform.* **2011**, *30*, 443−458.
(6) Cavalli, A.; Poluzzi, E.; De Ponti, F.; Recanatini, M. Toward a Pharmacophore for Drugs Inducing the Long QT Syndrome: Insights from a CoMFA Study of HERG K+ Channel Blockers. *J. Med. Chem.* **2002**, *45*, 3844−3853.
(7) Ekins, S.; Crumb, W. J.; Sarazan, R. D.; Wikel, J. H.; Wrighton, S. A. Three-Dimensional Quantitative Structure-Activity Relationship for Inhibition of Human Ether-a-Go-Go-Related Gene Potassium Channel. *J. Pharmacol. Exp. Ther.* **2002**, *301*, 427−434.
(8) Pearlstein, R. A.; Vaz, R. J.; Kang, J.; Chen, X.-L.; Preobrazhenskaya, M.; Shchekotikhin, A. E.; Korolev, A. M.; Lysenkova, L. N.; Miroshnikova, O. V.; Hendrix, J.; Rampe, D. Characterization of HERG potassium Channel Inhibition Using CoMSiA 3D QSAR and Homology Modeling Approaches. *Bioorg. Med. Chem. Lett.* **2003**, *13*, 1829−1835.
(9) Aronov, A. M.; Goldman, B. B. A Model for Identifying HERG K + Channel Blockers. *Bioorg. Med. Chem.* **2004**, *12*, 2307−2315.
(10) Aronov, A. M. Common Pharmacophores for Uncharged Human Ether-a-go-go-Related Gene (hERG) Blockers. *J. Med. Chem.* **2006**, *49*, 6917−6921.
(11) Jensen, M. O.; Jogini, V.; Borhani, D. W.; Leffler, A. E.; Dror, R. O.; Shaw, D. E. Mechanism of Voltage Gating in Potassium Channels. *Science* **2012**, *336*, 229−233.
(12) Mitcheson, J. S.; Chen, J.; Lin, M.; Culberson, C.; Sanguinetti, M. C. A Structural Basis for Drug-Induced Long QT Syndrome. *Proc. Natl. Acad. Sci. U. S. A.* **2000**, *97*, 12329−12333.
(13) Tseng, G.-N.; Sonawane, K. D.; Korolkova, Y. V.; Zhang, M.; Liu, J.; Grishin, E. V.; Guy, H. R. Probing the Outer Mouth Structure of the hERG Channel with Peptide Toxin Footprinting and Molecular Modeling. *Biophys. J.* **2007**, *92*, 3524−3540.
(14) Stansfeld, P. J.; Grottesi, A.; Sands, Z. A.; Sansom, M. S. P.; Gedeck, P.; Gosling, M.; Cox, B.; Stanfield, P. R.; Mitcheson, J. S.; Sutcliffe, M. J. Insight into the Mechanism of Inactivation and pH Sensitivity in Potassium Channels from Molecular Dynamics Simulations. *Biochemistry* **2008**, *47*, 7414−7422.
(15) Österberg, F.; Å qvist, J. Exploring Blocker Binding to a Homology Model of the Open hERG K+ Channel Using Docking and Molecular Dynamics Methods. *FEBS Lett.* **2005**, *579*, 2939−2944.
(16) Rajamani, R.; Tounge, B. A.; Li, J.; Reynolds, C. H. A Two-State Homology Model of the hERG K+ Channel: Application to Ligand Binding. *Bioorg. Med. Chem. Lett.* **2005**, *15*, 1737−1741.
(17) Kramer, C.; Beck, B.; Kriegl, J. M.; Clark, T. A Composite Model for hERG Blockade. *ChemMedChem.* **2008**, *3*, 254−265.

(18) Stary, A.; Wacker, S. J.; Boukharta, L.; Zachariae, U.; Karimi-Nejad, Y.; Å qvist, J.; Vriend, G.; de Groot, B. L. Toward a Consensus Model of the hERG Potassium Channel. *ChemMedChem.* **2010**, *5*, 455−467.
(19) Ng, C. A.; Perry, M. D.; Tan, P. S.; Hill, A. P.; Kuchel, P. W.; Vandenberg, J. I. The S4S5 Linker Acts as a Signal Integrator for hERG K^+ Channel Activation and Deactivation Gating. *PLoS One* **2012**, *7*, e31640.
(20) Durdagi, S.; Deshpande, S.; Duff, H. J.; Noskov, S. Y. Modeling of Open, Closed, and Open-Inactivated States of the hERG1 Channel: Structural Mechanisms of the State-Dependent Drug Binding. *J. Chem. Inf. Model.* **2012**, *52*, 2760−2774.
(21) Long, S. B.; Tao, X.; Campbell, E. B.; MacKinnon, R. Atomic Structure of a Voltage-Dependent K+ Channel in a Lipid Membrane-Like eEnvironment. *Nature* **2007**, *450*, 376.
(22) Di Martino, G. P.; Masetti, M.; Ceccarini, L.; Cavalli, A.; Recanatini, M. An Automated Docking Protocol for hERG Channel Blockers. *J. Chem. Inf. Model.* **2013**, *53*, 159−175.
(23) Long, S. B.; Tao, X.; Campbell, E. B.; MacKinnon, R. Atomic Structure of a Voltage-Dependent K+ Channel in a Lipid Membrane-Like Environment. *Nature* **2007**, *450*, 376−382.
(24) Humphrey, W.; Dalke, A.; Schulten, K. {VMD} − {V}isual {M}olecular {D}ynamics. *J. Mol. Graph.* **1996**, *14*, 33−38.
(25) Phillips, J. C.; Braun, R.; Wang, W.; Gumbart, J.; Tajkhorshid, E.; Villa, E.; Chipot, C.; Skeel, R. D.; Kalé, L.; Schulten, K. Scalable Molecular Dynamics with NAMD. *J. Comput. Chem.* **2005**, *26*, 1781−1802.
(26) MacKerell, A. D.; et al. All-Atom Empirical Potential for Molecular Modeling and Dynamics Studies of Proteins. *J. Phys. Chem. B* **1998**, *102*, 3586−3616.
(27) Mackerell, A. D.; Feig, M.; Brooks, C. L. Extending the Treatment of Backbone Energetics in Protein Force Fields: Limitations of Gas-Phase Quantum Mechanics in Reproducing Protein Conformational Distributions in Molecular Dynamics Simulations. *J. Comput. Chem.* **2004**, *25*, 1400−1415.
(28) Beglov, D.; Roux, B. Finite Representation of an Infinite Bulk System: Solvent Boundary Potential for Computer Simulations. *J. Chem. Phys.* **1994**, *100*, 9050−9063.
(29) Schlenkrich, M.; Brickmann, J.; MacKerell, A. D.; Karplus, J. M. In *Biological Membranes*; Merz, K. M., Roux, J. B., Eds.; Birkhauser: Boston, 1996; pp 31−81.
(30) Jorgensen, W. L.; Chandrasekhar, J.; Madura, J. D.; Impey, R. W.; Klein, M. L. Comparison of simple potential functions for simulating liquid water. *J. Chem. Phys.* **1983**, *79*, 926−936.
(31) Darden, T.; York, Y.; Pedersen, L. Particle Mesh Ewald: An Nlog(N) Method for Ewald Sums in Large Systems. *J. Chem. Phys.* **1993**, *98*, 10089−10092.
(32) Lindorff-Larsen, K.; Piana, S.; Palmo, K.; Maragakis, P.; Klepeis, J. L.; Dror, R. O.; Shaw, D. E. Improved Side-Chain Torsion Potentials for the Amber ff99SB Protein Force Field. *Proteins Struct. Funct. Bioinforma.* **2010**, *78*, 1950−1958.
(33) Sherman, W.; Day, T.; Jacobson, M. P.; Friesner, R. A.; Farid, R. Novel Procedure for Modeling Ligand/Receptor Induced Fit Effects. *J. Med. Chem.* **2006**, *49*, 534−553.
(34) Beglov, D.; Roux, B. An Integral Equation To Describe the Solvation of Polar Molecules in Liquid Water. *J. Phys. Chem. B* **1997**, *101*, 7821−7826.
(35) Kovalenko, A.; Hirata, F. Three-Dimensional Density Profiles of Water in Contact with a Solute of Arbitrary Shape: a RISM Approach. *Chem. Phys. Lett.* **1998**, *290*, 237−244.
(36) Labute, P. Protonate3D: Assignment of Ionization States and Hydrogen Coordinates to Macromolecular Structures. *Proteins Struct. Funct. Bioinforma.* **2009**, *75*, 187−205.
(37) Case, D.A.; et al. *Amber 12*; University of California, San Francisco, 2012.
(38) Dickson, C. J.; Rosso, L.; Betz, R. M.; Walker, R. C.; Gould, I. R. GAFFlipid: a General Amber Force Field for the Accurate Molecular Dynamics Simulation of Phospholipid. *Soft Matter* **2012**, *8*, 9617−9627.
(39) Domanski, J.; Stansfeld, P.; Sansom, M.; Beckstein, O. Lipidbook: A Public Repository for Force-Field Parameters Used in Membrane Simulations. *J. Membr. Biol.* **2010**, *236*, 255−258.
(40) Fernandez, D.; Ghanta, A.; Kauffman, G. W.; Sanguinetti, M. C. Physicochemical Features of the hERG Channel Drug Binding Site. *J. Biol. Chem.* **2004**, *279*, 10120−10127.
(41) Stansfeld, P. J.; Sutcliffe, M. J.; Mitcheson, J. S. Molecular Mechanisms for Drug Interactions with hERG that Cause Long QT Syndrome. *Expert Opin. Drug Metab. Toxicol.* **2006**, *2*, 81−94.
(42) Schmidtke, P.; Bidon-Chanal, A.; Luque, F. J.; Barril, X. MDpocket: Open-Source Cavity Detection and Characterization on Molecular Dynamics Trajectories. *Bioinformatics* **2011**, *27*, 3276−85.
(43) Stepanovic, S. Z.; Potet, F.; Petersen, C. I.; Smith, J. A.; Meiler, J.; Balser, J. R.; Kupershmidt, S. The Evolutionarily Conserved Residue A653 Plays a Key Role in HERG Channel Closing. *J. Physiol.* **2009**, *587*, 2555−2566.
(44) Bian, J.-S.; Cui, J.; Melman, Y.; McDonald, T. S641 Contributes HERG K+ Channel Inactivation. *Cell Biochem. Biophys.* **2004**, *41*, 25−39.
(45) Ju, P.; Pages, G.; Riek, R. P.; Chen, P.-c.; Torres, A. M.; Bansal, P. S.; Kuyucak, S.; Kuchel, P. W.; Vandenberg, J. I. The Pore Domain Outer Helix Contributes to Both Activation and Inactivation of the hERG K+ Channel. *J. Biol. Chem.* **2009**, *284*, 1000−1008.
(46) Koepfer, D. A.; Hahn, U.; Ohmert, I.; Vriend, G.; Pongs, O.; de Groot, B. L.; Zachariae, U. A Molecular Switch Driving Inactivation in the Cardiac K+ Channel hERG. *PLoS One* **2012**, *7*, e41023.
(47) Lees-Miller, J. P.; Subbotina, J. O.; Guo, J.; Yarov-Yarovoy, V.; Noskov, S. Y.; Duff, H. J. Interactions of H562 in the S5 Helix with T618 and S621 in the Pore Helix Are Important Determinants of hERG1 Potassium Channel Structure and Function. *Biophys. J.* **2009**, *96*, 3600−3610.
(48) Farid, R.; Day, T.; Friesner, R. A.; Pearlstein, R. A. New Insights about HERG Blockade Obtained from Protein Modeling, Potential Energy Mapping, and Docking Studies. *Bioorg. Med. Chem.* **2006**, *14*, 3160−3173.
(49) Zachariae, U.; Giordanetto, F.; Leach, A. G. Side Chain Flexibilities in the Human Ether-a-go-go Related Gene Potassium Channel (hERG) Together with Matched-Pair Binding Studies Suggest a New Binding Mode for Channel Blockers. *J. Med. Chem.* **2009**, *52*, 4266−4276.
(50) Boukharta, L.; Keranen, H.; Stary-Weinzinger, A.; Wallin, G.; de Groot, B. L.; Å qvist, J. Computer Simulations of StructureActivity Relationships for hERG Channel Blockers. *Biochemistry* **2011**, *50*, 6146−6156.
(51) Perry, M.; Sachse, F. B.; Sanguinetti, M. C. Structural Basis of Action for a Human Ether-a-go-Ggo-Related Gene 1 Potassium Channel Activator. *Proc. Natl. Acad. Sci. U. S. A.* **2007**, *104*, 13827−13832.
(52) Halgren, T. A.; Murphy, R. B.; Friesner, R. A.; Beard, H. S.; Frye, L. L.; Pollard, W. T.; Banks, J. L. Glide: a New Approach for Rapid, Accurate Docking and Scoring. 2. Enrichment Factors in Database Screening. *J. Med. Chem.* **2004**, *47*, 1750−1759.
(53) Myokai, T.; Ryu, S.; Shimizu, H.; Oiki, S. Topological Mapping of the Asymmetric Drug Binding to the Human Ether-à-go-go-Related Gene Product (HERG) Potassium Channel by Use of Tandem Dimers. *Mol. Pharmacol.* **2008**, *73*, 1643−1651.
(54) Truchon, J.-F.; Bayly, C. I. Evaluating Virtual Screening Methods: Good and Bad Metrics for the Early Recognition Problem. *J. Chem. Inf. Model.* **2007**, *47*, 488−508.
(55) Dougherty, D. A. Cation-π Interactions in Chemistry and Biology: A New View of Benzene, Phe, Tyr, and Trp. *Science* **1996**, *271*, 163−168.
(56) Gallivan, J. P.; Dougherty, D. A. Cation-π Interactions in Structural Biology. *Proc. Natl. Acad. Sci. U. S. A.* **1999**, *96*, 9459−9464.
(57) Aronov, A. M. Tuning out of hERG. *Curr. Opin. Drug Discovery Devel.* **2008**, *11*, 128.
(58) Thai, K.-M.; Ecker, G. F. A Binary QSAR Model for Classification of hERG Potassium Channel Blockers. *Bioorg. Med. Chem.* **2008**, *16*, 4107−4119.

(59) Dubus, E.; Ijjaali, I.; Petitet, F.; Michel, A. In Silico Classification of hERG Channel Blockers: a Knowledge-Based Strategy. *ChemMedChem.* **2006**, *1*, 622−630.
(60) Garg, V.; Stary-Weinzinger, A.; Sachse, F.; Sanguinetti, M. C. Molecular Determinants for Activation of Human Ether-à-go-go-related Gene 1 Potassium Channels by 3-Nitro-N-(4-phenoxyphenyl) Benzamide. *Mol. Pharmacol.* **2011**, *80*, 630−637.

■ NOTE ADDED AFTER ASAP PUBLICATION

This article was published ASAP on July 18, 2014. Additional content was added to the Supporting Information. The corrected version was published ASAP on August 8, 2014.